PERGAMON

International Journal of Multiphase Flow 26 (2000) 45–66

International Journal of Multiphase Flow

www.elsevier.com/locate/ijmulflow

The behaviour of gas bubbles in a turbulent liquid metal magnetohydrodynamic flow Part I: Dispersion in quasi-two-dimensional magnetohydrodynamic turbulence

S. Eckert[a,*], G. Gerbeth[a], O. Lielausis[b]

[a]*Forschungszentrum Rossendorf (FZR), P.O. Box 510119, 01314 Dresden, Germany*
[b]*Latvian Academy of Science, Institute of Physics (LAS-IFP), 2169 Salaspils-1, Miera iela 32, Latvia*

Received 18 December 1997; received in revised form 13 January 1999

Abstract

We investigate the dispersion of gas bubbles injected from a single orifice into a liquid metal flow subjected to transverse and longitudinal magnetic fields. The local void fraction is detected by means of resistivity probes. The results show a damping of velocity fluctuations corresponding to a decrease in the bubble dispersion with increasing magnetic field. An isotropic distribution of the gas phase is preserved if a longitudinal field is applied, while an anisotropic distribution is observed in case the applied magnetic field is transverse to the flow indicating the existence of quasi-two-dimensional vortices as typical of turbulent magnetohydrodynamic flows. © 1999 Elsevier Science Ltd. All rights reserved.

Keywords: Liquid metal–gas flow; Bubble; Magnetic field; MHD turbulence; Void fraction; Resistivity probe

1. Introduction

In the last few decades magnetohydrodynamic (MHD) effects have attracted growing interest because of its potential impact on numerous industrial technologies. In processes involving electrically conducting liquids, the application of an external magnetic field offers opportunities for a contactless flow control and fluid handling. Steady fields are suitable for suppressing instabilities. Time-dependent fields allow a selective generation of a large variety of flow

* Corresponding author.

PII: S0301-9322(99)00006-3

structures. Thus, in metallurgy electromagnetic pumping or mixing can be as effective as conventional technologies. Injected gas bubbles are used in many technologies in order to drive some liquid motion or to enhance transport processes. One has to look for suitable methods to control the properties of such flows. The utilization of a magnetic field seems to be an attractive way to affect the distribution of the bubbles or the momentum transfer between the gas and the liquid. Therefore, the interest of this paper is focused on the interaction of a turbulent liquid metal flow containing small gas bubbles with an external steady magnetic field. The following part I of the paper deals with the dispersion of gas bubbles in a turbulent MHD flow, while in part II the influence of an external magnetic field on the relative motion of the gas in the liquid metal flow, i.e. on the slip ratio, is considered.

Little is known about the local turbulence structure of MHD two-phase flows. In fact, theoretical approaches are confronted with remarkable difficulties due to the complexity and the statistical character of two-phase flows combined with the special features arising from the additional electromagnetic force. On the experimental side, the application of measuring techniques well-tried in ordinary hydrodynamics to liquid metals or alloys is seriously impeded by the nature of such fluids (nontransparent, abrasive, high temperatures).

Considering an electrically conducting, single-phase fluid the application of a strong magnetic field leads to a reorganization of the mean flow as well as to a modification of the local turbulence structure. The electromagnetic damping caused by the Lorentz force $\vec{j} \times \vec{B}$ is an important feature of MHD flows leading to an additional anisotropic Joule dissipation term in the Navier–Stokes equation. Consequently, the magnitude of the electromagnetic dissipation experienced by a vortex depends on the direction of its vorticity vector. Vortices having an axis aligned with the magnetic field lines are primarily not affected by electromagnetic damping, while vortices with vorticity vectors perpendicular to the field are damped rather quickly. This results in a significant anisotropy of the turbulent fluctuations. MHD turbulence can become quasi-two-dimensional under the supposition of strong magnetic fields and suitable boundary conditions (Sommeria and Moreau, 1982). As known from the two-dimensional turbulence theory (Kraichnan, 1967), the usual direct energy cascade towards small scales is replaced by an inverse energy cascade towards large scales and a simultaneous transfer of enstrophy (vorticity squared) towards high wavenumber perturbations. Thus, the kinetic energy becomes concentrated in well-organised large-scale fluctuations characterised by a long decay time. Measurements in MHD channel flows revealed that quasi-two-dimensional turbulent fluctuations survive in such flows although the overall pressure-drop beyond a critical ratio of Hartmann to Reynolds number corresponds to laminar flow values. See Moreau (1990) for more details and corresponding references.

While the direct influence of the magnetic field on the local properties of turbulence has already been studied in sufficient depth, the transport processes of mass and heat in turbulent MHD flows are not yet sufficiently understood. The specific properties of two-dimensional MHD turbulence give reason to suppose that the Reynolds analogy between momentum transfer and transport of a passive scalar, which is well-known in ordinary hydrodynamics, is not valid for the MHD case. By means of a well-aimed excitation of quasi-two-dimensional vortices an enhancement of the transfer properties should be reached without a corresponding rise of the pressure losses. For instance, Kolesnikov and Tsinober (1974) used a mechanical grid installed in the channel cross section to promote the generation of velocity fluctuations in

a mercury flow. They injected an indium–mercury solution into the mercury flow and analysed the local amount of indium along the lines parallel and transverse to the magnetic field direction. If no magnetic field was applied to the flow, the mass transfer remains practically symmetric in both directions, whereas in the presence of a strong magnetic field the mass transfer decreases very sharply along the field lines and increases in the perpendicular direction.

Now the question arises, can similar results be expected for the dispersion of gas bubbles? However, alone the problem of the turbulent motion of bubbles in a liquid is rather difficult. The interaction between a turbulent flow and dispersed gas bubbles, especially the effect of the turbulent flow structure of the carrier phase on the bubble trajectories, has already been considered by several investigators (for example, Taylor, 1934; Hinze, 1955; Sevik and Park, 1973). The turbulence observed in two-phase flows should be interpreted as a superposition of velocity fluctuations originated from different sources: the shear layers in the mean flow, the irregular movement of the gas inclusions, and the turbulent wakes of the gas bubbles. Thus, the turbulence intensity in a two-phase flow is expected to be higher compared to the corresponding value for the single-phase flow at the same superficial velocity. This was confirmed experimentally by several authors (Serizawa et al., 1975a, 1975b and 1975c; Sullivan et al., 1978; Ohba and Yuhara, 1979) for two-phase flows with relative high void fractions ($\epsilon \approx 10$–30%). In the case of rising bubbles in a stagnant fluid with a small gas content ($\epsilon \approx 1$–2%), an increase of the turbulence intensity proportional to the square root of the void fraction was found by Michiyoshi and Serizawa (1984), and Gherson and Lykoudis (1984). This dependence was also shown in the MHD case for void fractions up to 6.5% by Lykoudis et al. (1994).

The first experiments about the properties of a two-phase flow exposed to a magnetic field was reported by Thome (1964). Dunn (1980) presented results of pressure-difference and wall-voltage measurements for a vertically downward pipe flow in a transverse magnetic field. Local measurements were not included in both the papers. Up to the present time a growing number of publications dealing with investigations of the local structure of MHD two-phase flows can be noted. For instance, measured void fraction profiles are presented by Lykoudis (1985), Michiyoshi (1989), Michiyoshi et al. (1977), Saito et al. (1978a) and Serizawa et al. (1990). Mori et al. (1977) investigated the velocity of rising bubbles in a mercury tank exposed to a horizontal magnetic field using multi-wire resistivity probes. Serizawa et al. (1990) reported the influence of a magnetic field on flow regime transitions.

Fabris et al. (1980), and Gherson and Lykoudis (1984) measured the local liquid velocity and their fluctuating part in an MHD two-phase flow by means of hot-film probes. From a qualitative evaluation of the velocity fluctuation signal Fabris et al. (1980) found that for two-phase flows the fluctuations appear to increase in magnitude with increasing B, while for pure-liquid flows the velocity perturbations are damped. In parallel, a decrease of the bubble number with increasing field strength is observed, which has been explained by a breakup of the bubbles due to the magnetic field action. As a result, most of the bubbles are too small to be detectable by the local sensor. In contrast to this interpretation, Serizawa et al. (1990) found a tendency to enhance the bubble coalescence in the MHD case. Gherson and Lykoudis (1984) calculated power spectra from the velocity fluctuation signals. However, one is confronted with considerable difficulties clearly to distinguish between the parts of the signal corresponding to the liquid and to the dispersed gas phase, respectively. Moreover, the mathematical techniques

to evaluate the autocorrelation and power spectrum of the continuous phase signals in dispersed two-phase flows are important points of discussion up to now (see Panidis, 1995).

In summary one has to note that a uniform, consistent picture about the local structure of turbulent MHD two-phase flows does not exist. Unfortunately, most of the above mentioned studies have been performed in tubes with a circular cross section which offer poor conditions for the formation of quasi-two-dimensional turbulence (Moreau, 1990). Mainly, high values of the void fraction up to 80% have been considered leading to a flow regime pattern beyond the bubbly flow. Moreover, the magnetic field strength, and connected with it the corresponding dimensionless parameter Ha and N, was only modified in few steps, sometimes only a comparison between $B = 0$ and $B \neq 0$ has been presented. The use of sodium with its favourable material properties (high electrical conductivity, low kinematic viscosity) allows us to reach parameter regions of high Hartmann numbers ($Ha_{\max} = 2700$) and interaction parameters ($N_{\max} = 800$) with rather moderate magnetic field strengths. This is an important advantage compared to the papers published so far. Our goal here is to investigate the influence of an external magnetic field on the dispersion of gas bubbles in a broad range of Hartmann and Stuart numbers.

In Section 2 of this paper the main features of the experimental facilities will be presented (Section 2.1). Moreover, the reader will find some estimations regarding the flow situation which can be expected for the given experimental configuration in Section 2.2 and a brief description of the measuring technique in Section 2.3. The presentation of the experimental results will follow considering the distributions of the local void fraction in Section 3 and the derived dispersion coefficients in Section 4, respectively.

2. Experimental considerations

2.1. Experimental setup

Because the requirements for the existence of quasi-two-dimensional turbulence in channel flows are met if the magnetic field is directed transverse to the flow, this paper centres on the investigations with the applied transverse magnetic field at the sodium/argon-facility of the Forschungszentrum Rossendorf (FZR). Nevertheless, to complement the picture it is interesting to compare these results with corresponding measurements obtained in a longitudinal field configuration. An electromagnet system providing such a longitudinal magnetic field is not available at the experimental loop in Rossendorf. Therefore, the mercury/nitrogen-facility of the Institute of Physics in Riga (IfP) is used to perform these measurements. This comparison should be considered more qualitatively, because the employment of a different fluid combination, which in general gives no problems from the physical point of view, does not allow us to reach exactly the same parameter regions.

The experimental configurations are very similar and can be characterised as follows: the gas phase is injected into a vertical, upstreaming liquid metal by a single orifice located in the centre of the channel cross section (see Fig. 1). The flow is exposed to an external magnetic field directed transverse or longitudinal to the mean flow direction. After a distinct distance the local void fraction is measured by means of resistivity probes. This kind of sensors, which

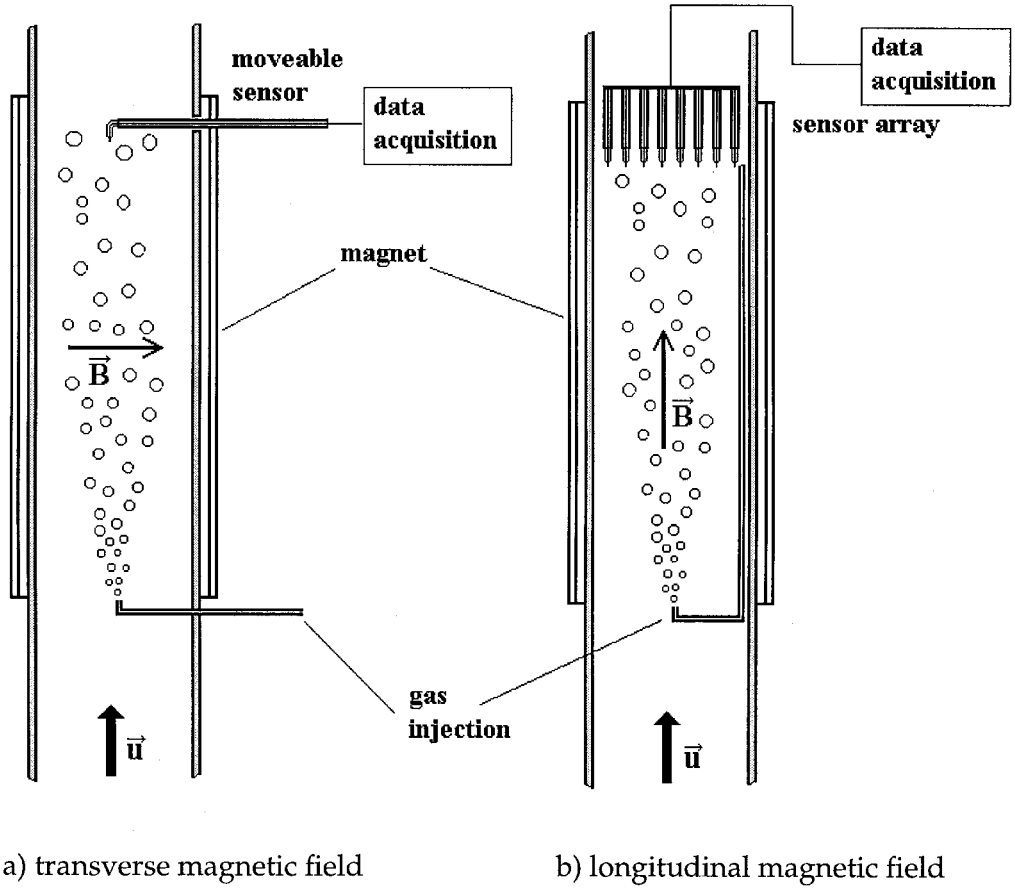

Fig. 1. Simplified scheme of the vertical two-phase test sections.

represents a standard measuring technique in ordinary two-phase flow (see, for example, Jones and Delhaye, 1976), has been adapted to liquid metal (especially sodium) flows. Potential-difference probes (as described by Branover, 1978) capable for measuring local velocities in the case of MHD flows are applied at the sodium facility in order to determine the turbulence intensity.

2.1.1. Sodium loop (sodium–argon flow, transverse magnetic field, Fig. 2)

The facility operates with a sodium–argon flow in a vertical test section with a cross-sectional area of 45×50 mm^2. The mean flow is generated by an electromagnetic pump and passes a transverse magnetic field (length: 320 mm, B_{max}: 0.45 T). The channel half-width in the direction of the transverse magnetic field will be designated with a, while b stands for the channel half-width in the direction perpendicular to the field. An electromagnetic flow meter is used in order to determine the sodium flow rate.

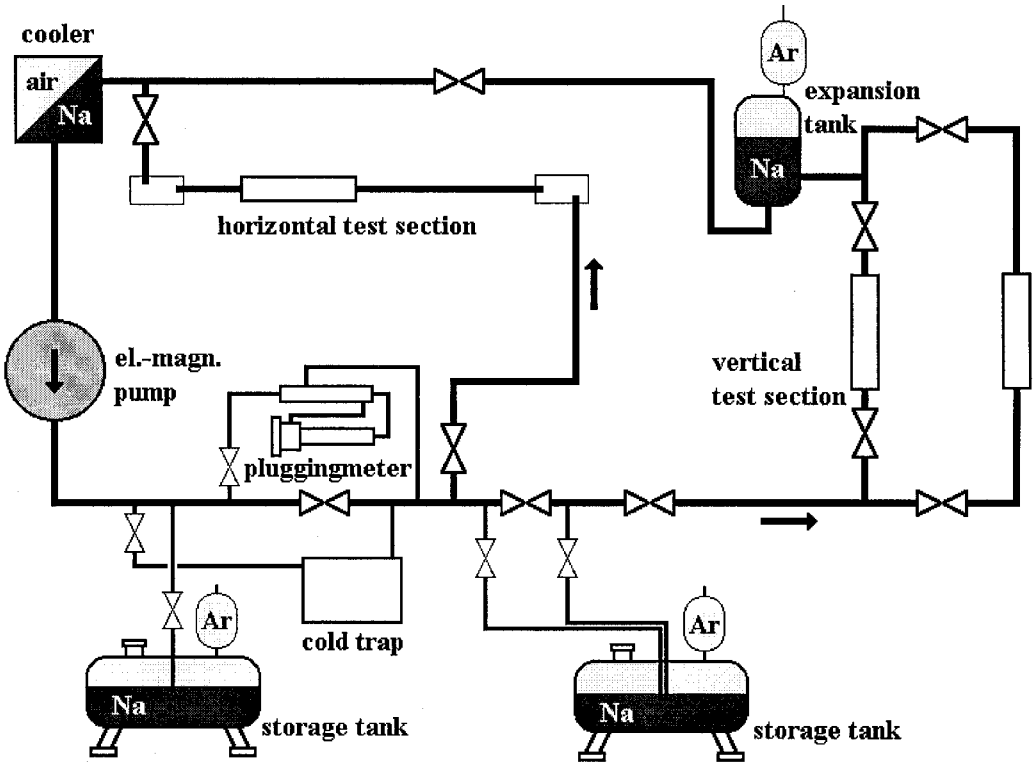

Fig. 2. Schematic view of the FZR sodium facility.

The channel wall thickness of $\delta_w = 3$ mm leads to a wall conductance ratio of $c_w = \sigma_{el,w} \cdot \delta_w/\sigma_{el,L} \cdot a = 0.026$ ($\sigma_{el,w}$ is the electrical conductivity of the channel wall, $\sigma_{el,L}$ is electrical conductivity of the liquid). At the smallest Hartmann number of $Ha = 300$ (definition of the Hartmann number is given in the next section) used in the experiment ($B = 0.05$ T) we obtain for the ratio of the electric resistances of the Hartmann layer and the channel wall $R_{Ha}/R_w = Ha \cdot c_w$ a value of 3.9. Therefore, one has to practically deal with the case of conducting walls. That means the closure of the electric current induced by the interaction of the flow with the magnetic field takes place over the channel wall and, as result, a significant electromagnetic damping effect on the turbulent fluctuations has to be expected.

The gas bubbles are injected by a single orifice ($\varnothing$ 0.8 mm) installed just at the beginning of the magnetic pole face region. A small volumetric quality β ($\beta = \dot{Q}_G/\dot{Q}_G + \dot{Q}_L = 0.05$–$0.09$; $\dot{Q}_G$, $\dot{Q}_L$ volumetric flow rates of gas and liquid, respectively) is selected in order to guarantee a pure bubbly flow regime.

The measuring probes are connected with a traversing mechanism to move the sensor over the cross-sectional area.

2.1.2. Mercury loop (mercury–nitrogen, longitudinal magnetic field, Fig. 3)

The test section of the mercury facility consists of a vertical tube 100 mm in diameter with an entire length of 4 m. The longitudinal magnetic field is provided by a solenoid (length: 2 m,

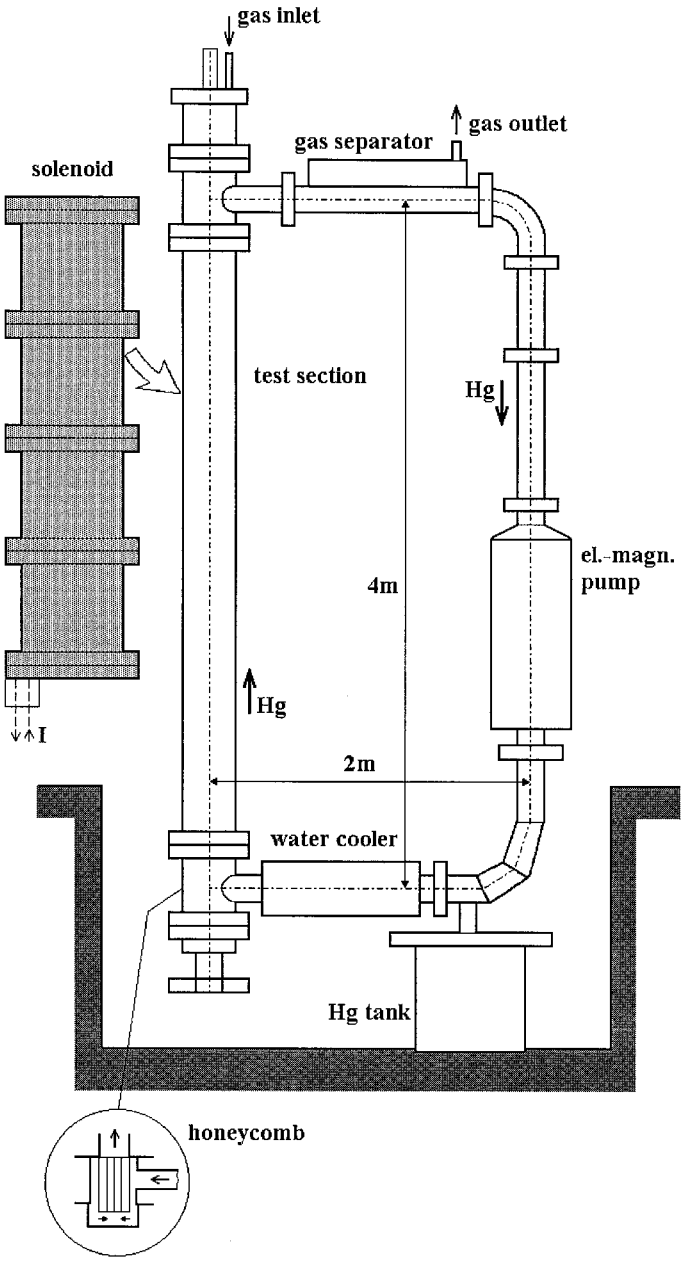

Fig. 3. Schematic view of the IFP mercury loop.

B_{max}: 0.9 T). An electromagnetic pump is employed in order to drive the liquid metal. The adjustable maximum of the mercury inlet velocity is 0.18 m/s corresponding to a Reynolds number of about 163000. The liquid flow rate is measured by means of a venturi flow meter.

At the entrance of the single-phase flow into the vertical test section a honeycomb is

installed with the aim to adjust a uniform flow profile. The bubbles are injected above this honeycomb by a single orifice (⌀ 1.2 mm). The distance between the gas injection and the probe location can be chosen in the range from 0.2 to 1.5 m. Sixteen individual probes are mounted at a cross-shaped frame in such a manner that every sensor is installed at a different radial distance from the centre of the channel cross section. This frame can be rotated as well as translated in axial direction.

2.2. Estimated flow characteristics

2.2.1. Turbulence structure

Crucial parameters of the MHD case are the Hartmann number Ha describing the ratio between electromagnetic and viscous forces and the Stuart number N describing the ratio between electromagnetic and inertial forces:

$$Ha = BL\sqrt{\frac{\sigma_{\mathrm{el}}}{\eta}} \tag{1}$$

$$N = \frac{\sigma_{\mathrm{el}} L B^2}{\rho V} = \frac{Ha^2}{Re} \tag{2}$$

where $B,L,V,\rho,\sigma_{\mathrm{el}},\eta$ stand for the magnetic field induction, typical length scale, typical velocity scale, density, electrical conductivity, and dynamic viscosity of the fluid, respectively. The measurements were performed in a parameter range ($Ha \gg 1, N > 1$), where the local structure of the turbulent sodium flow is strongly influenced by the applied magnetic field.

Branover (1978) evaluated a number of early experimental results obtained in the sixties and seventies considering turbulent channel flows in transverse fields. The following empirical relation given by him delivers a critical ratio of Hartmann to Reynolds number denoting a rough indication for the minimal field strength, when the overall pressure drop begins to follow the theoretical curve for a laminar MHD flow:

$$\left(\frac{Ha}{Re}\right)_{\mathrm{cr}} = \left[215 - 85 \cdot \mathrm{e}^{-0.35 \cdot A_{\mathrm{r}}}\right]^{-1} \quad ; \quad A_{\mathrm{r}} = \frac{b}{a} \tag{3}$$

A channel aspect ratio A_{r} of about 1 leads to a critical value of 7×10^{-3}. This value has been reached and clearly exceeded in our experiments.

Eckert (1997) performed local measurements of the longitudinal sodium velocity component and their fluctuating part by means of potential probes in order to characterise the properties of the sodium single-phase flow under the same experimental conditions (test section, nondimensional parameters).

These results will be published elsewhere and shall be briefly summarised here: the mean velocity profile becomes more and more M-shaped for increasing Hartmann numbers. The reason is the presence of conducting channel walls and, moreover, the inhomogeneity of the magnetic field strength in the end regions of the pole faces. For Stuart numbers $N < 10$ turbulence intensities were found between 3% and 4%. A further increase in the field strength causes a decrease of the turbulence intensity to values less than 1%. This fact becomes also

obvious in the calculated power spectra. The turbulent kinetic energy is damped with growing magnetic field. A significant enhancement of the turbulence is reached by the installation of a suitable turbulence promoter in the cross-sectional area just at the beginning of the magnetic field. With a grid consisting of four cylindrical bars directed parallel to the magnetic field lines turbulence intensities up to 15% were measured for Stuart numbers of about 100. These results are in qualitative agreement with those of Branover et al. (1994), also cover higher values of Ha and N.

2.2.2. Two-phase flow

Our experiments employ small void fractions ($\epsilon < 5\%$) in order to keep the bubble-induced turbulence small. Moreover, the restriction to low gas flow rates should guarantee the formation of nearly spherical gas bubbles.

In order to estimate the bubble size and shape we use the Eotvos number Eo and the Morton number Mo

$$Eo = \frac{g\Delta\rho d_b^2}{\sigma} \tag{4}$$

$$Mo = \frac{g\eta^4\Delta\rho}{\rho^2\sigma^3} \tag{5}$$

where d_b,ρ,σ,η and g stand for diameter of the bubble, density, surface tension, dynamic viscosity of the fluid and gravitational acceleration, respectively.

For large fluid containers, an estimation for the ratio of vertical to horizontal bubble perimeter $\bar{E}$ is given by the relation (Clift et al., 1978):

$$\bar{E} = 1/\left(1 + 0.163 \cdot Eo^{0.757}\right) \quad Eo < 40,\ Mo \leq 10^{-6} \tag{6}$$

For a sodium flow at a temperature of 200°C we obtain the following values:

Morton number	7.3×10^{-14}
Eotvos number	2 ($d_b = 7$ mm) 0.2 ($d_b = 2$ mm)
$\bar{E}$	0.78 ($d_b = 7$ mm) 0.96 ($d_b = 2$ mm)

The same estimates deliver for mercury at room temperature:

Morton number	3.6×10^{-14}
Eotvos number	14 ($d_b = 7$ mm) 1.1 ($d_b = 2$ mm)
$\bar{E}$	0.45 ($d_b = 7$ mm) 0.85 ($d_b = 2$ mm)

According to these results only bubbles with a diameter of 2 mm in sodium can be considered as spherical, whereas bubbles in mercury will always more deviate from the spherical shape compared to sodium.

To estimate the bubble size we consider a single orifice with diameter d_k immersed in an infinite fluid. Under the assumptions of a constant bubble drag coefficient and negligible

inertial forces the following equation is obtained (see Brauer, 1971)

$$d_b = \left\{ \frac{3\sigma d_k}{g\rho} + \left[\left(\frac{3\sigma d_k}{g\rho} \right)^2 + \frac{15\dot{Q}_G^2 d_k}{g} \right]^{1/2} \right\}^{1/3} \tag{7}$$

In both types of experiments a typical gas flow rate of $\dot{Q}_G = 30$ l/h is used leading to bubble diameters of approximately 7 mm. That means, we have to note considerable deviations from the spherical bubble shape, particularly in the mercury experiment. However, any lowering of $\dot{Q}_G$ to inject smaller, spherical bubbles would cause an enormous prolongation of the measuring time. In order to ensure a small statistical error (< 10%) we accept the deviations from the spherical shape.

2.3. Data analysis

2.3.1. Void-fraction measurements

The resistivity probes are local sensors with an electrically conducting tip (Cr/Ni wire, ⌀ 0.1 mm) in direct contact with the liquid metal. The probe is supplied with an alternating current (1–10 kHz), which results in an electric current flowing from the probe tip to their hull pipe acting as the other electrode. The gas contact at the probe wire is detected by an interruption of the current. Due to the huge differences in the electrical conductivity between the gas and the liquid metal, we obtain very sharp signals easy to evaluate by a threshold method.

What we really measure is the local ratio of the gas contact time t_g to the total sampling time T, that means the time averaged local void fraction

$$\epsilon(\vec{r}) = \frac{1}{T}\int_0^T X(\vec{r},t)\,\mathrm{d}t = \frac{\sum_{m=1}^{M} t_{g,m}}{T} = \frac{t_G}{T} \tag{8}$$

where

$X(\vec{r},t) = 0$ in the case of contact with the liquid metal

$X(\vec{r},t) = 1$ in the case of gas contact

Here M is the total number of gas bubbles detected during the sampling time. Values of ϵ are measured at approximately 70 positions in the channel cross section. The shape of the function ϵ between these positions is obtained by interpolation.

Due to the statistical character of the two-phase flow, it is necessary to sample for a sufficiently long time in order to get a time-averaged value of the local void fraction of sufficient accuracy. In our case recording times of 200 s and more lead to relative measuring errors of about 2–10% depending on the bubble impact rate. Thus, a good compromise between accuracy and duration of the measurements was achieved.

2.3.2. Turbulence intensity measurements

The function of the potential-difference probe is governed by the Ohm's law in moving fluids. For MHD channel flows characterised by high Hartmann numbers and a small wall conductance ratio c_w ($1/Ha \ll c_w \ll 1$) the total current density $\vec{j}$ can be neglected compared to the induced one (a detailed discussion about the reliability of this measuring technique is given by Eckert (1997)):

$$|\vec{j}| \ll \sigma_{el}|(\vec{u} \times \vec{B})| \tag{9}$$

As a consequence, the measured electric potential drop $\Delta\phi$ between the electrodes, spatially separated by the distance l, has the following simple dependence on the fluid velocity (see also Fig. 4):

$$\Delta\phi = B \cdot l \cdot u \tag{10}$$

The presented values of the turbulence intensity tu are obtained from measurements of the time-averaged streamwise velocity component $\bar{u}$ and its fluctuating part u' according to the following relation:

$$tu = \frac{u'}{\bar{u}}, \quad u' = \left[\frac{1}{M-1}\sum_{m=1}^{M}(u_m - \bar{u})^2\right]^{1/2} \tag{11}$$

where M denotes here the total number of the sampled velocity values.

3. Distributions of local void fraction

3.1. Transverse magnetic field

Representative isoplots of the void fraction distribution in the cross-sectional area obtained

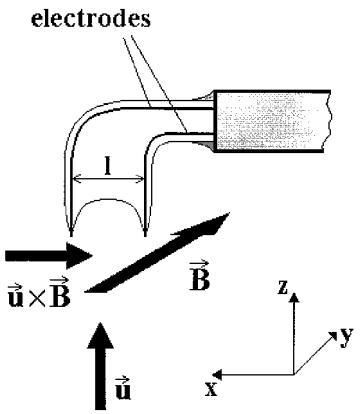

Fig. 4. Principle of the potential-difference probe to measure the local fluid velocity.

at different Reynolds numbers and different values of the magnetic field are displayed in Figs. 5–8.

In the ordinary hydrodynamic case without magnetic field (see Figs. 6a and 8a) the void fraction shows a distinct tendency to a uniform distribution over the cross-sectional area. However, the application of a small magnetic field ($B = 0.05$ T) causes a concentration of the

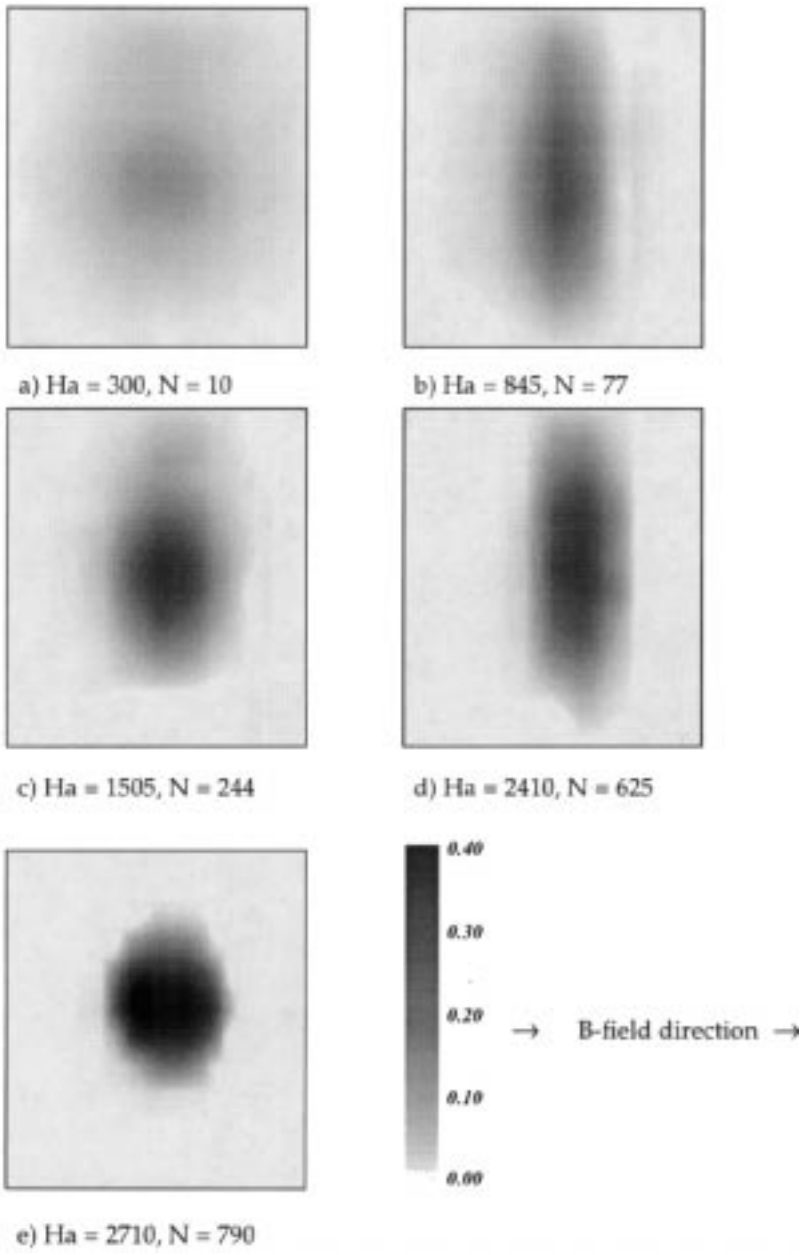

Fig. 5. Distributions of the local void fraction ϵ (%) at $Re = 9300$ (transverse magnetic field).

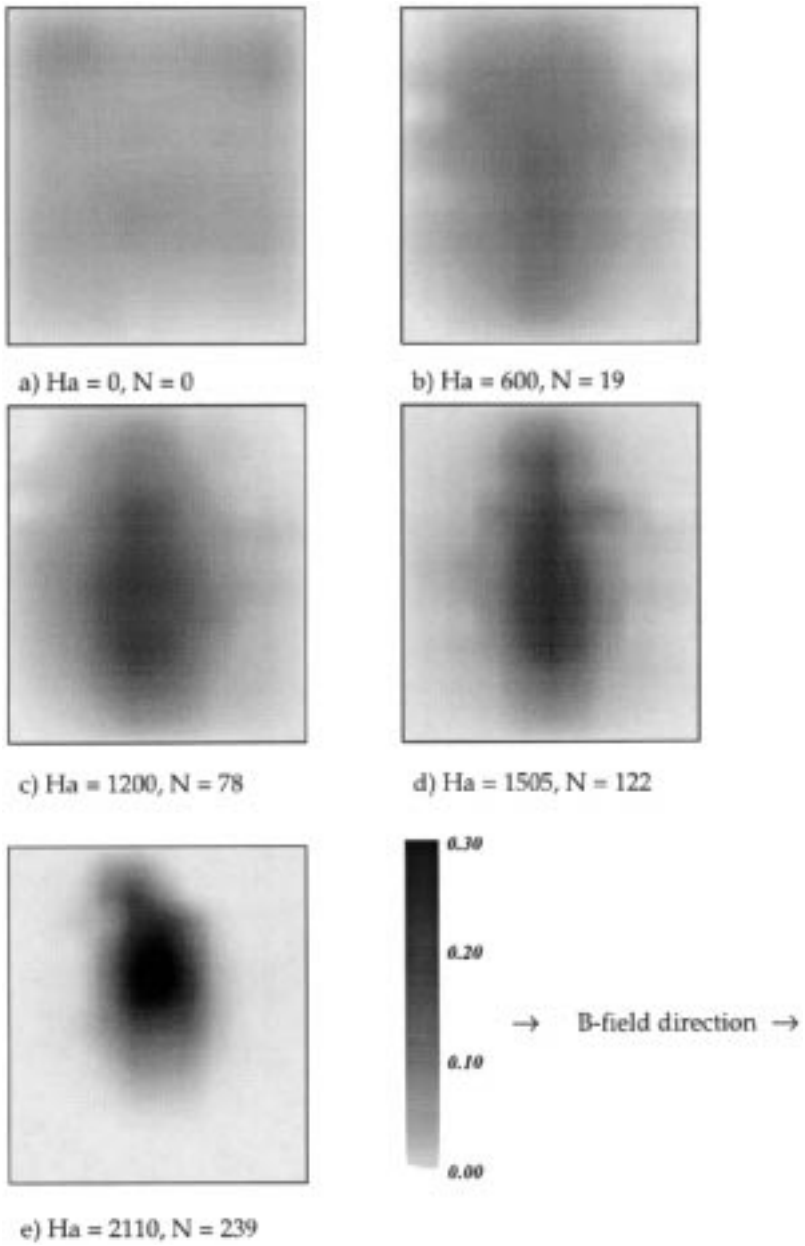

Fig. 6. Distributions of the local void fraction ϵ (%) at $Re = 18600$ (transverse magnetic field).

gas bubbles in the channel centre (Fig. 5a) indicating the damping of the turbulent fluctuations by the Lorentz force. The concentration process advances further with increasing magnetic field. If the Stuart number N exceeds a value of about 10, a significant anisotropy of the void fraction distribution is observed. The suppression of the bubble dispersion is much more pronounced in the direction parallel to the magnetic field lines than perpendicular it. This

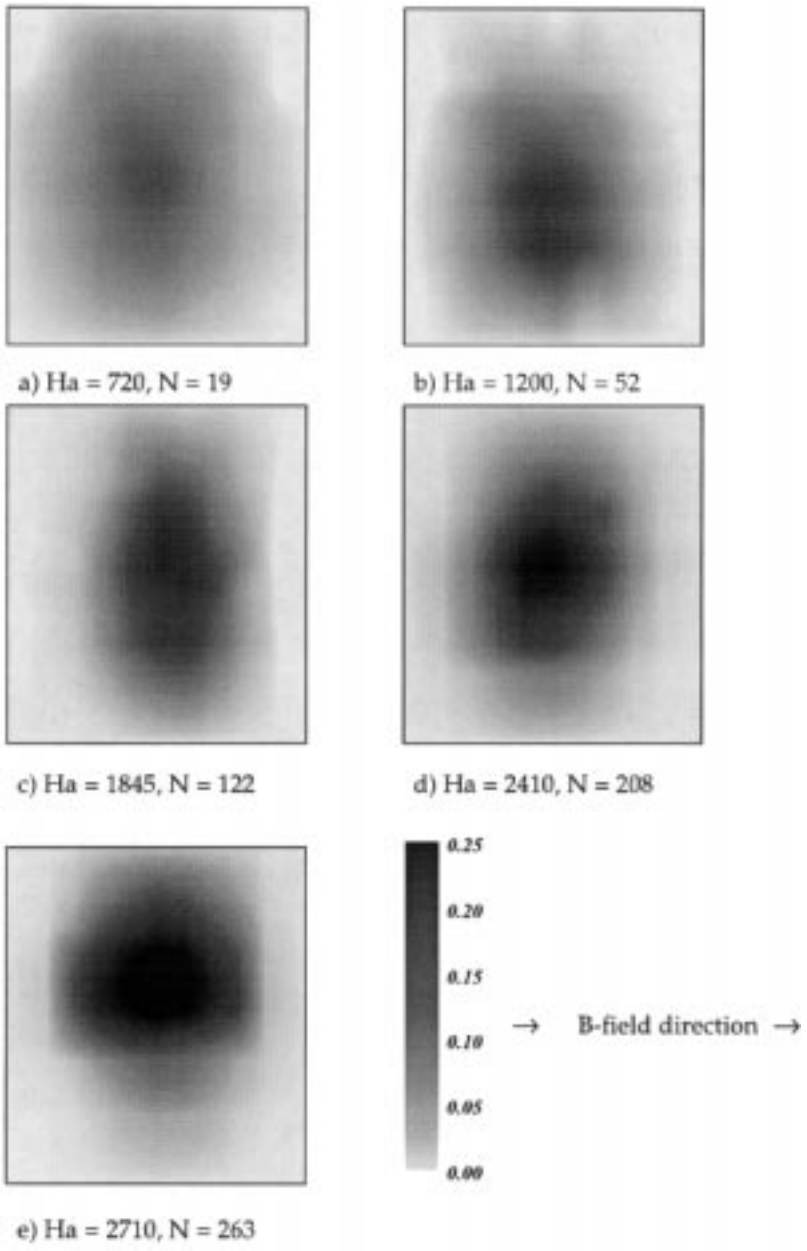

Fig. 7. Distributions of the local void fraction ϵ (%) at $Re = 27900$ (transverse magnetic field).

indicates the preferred existence of vortices with axes being aligned with the field direction. The character of the turbulent flow becomes more and more two dimensional.

For a Stuart number $N \geq 700$ (Fig. 5e) the gas phase is exclusively detected in the central region of the channel cross section. The distribution is again nearly isotropic, i.e. the two-

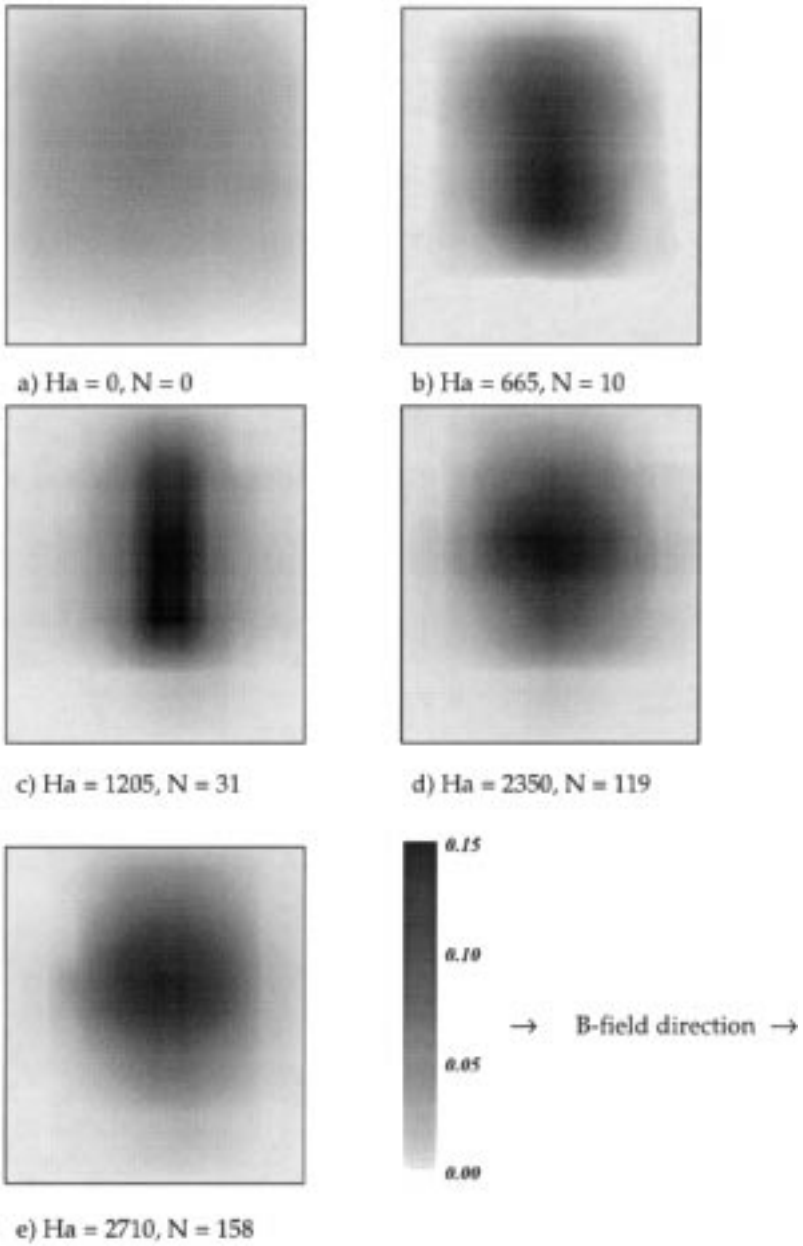

Fig. 8. Distributions of the local void fraction ϵ (%) at $Re = 46500$ (transverse magnetic field).

dimensional disturbances are damped by a sufficiently large magnetic field. As a result the flow becomes relaminarised.

Let us compare our results to the findings reported by Lykoudis (1985) and Michiyoshi (1989). They obtained an almost isotropic distribution in both directions perpendicular and parallel to the magnetic field. For some cases Lykoudis (1985) the gas phase is even more

concentrated in the perpendicular direction to the magnetic field. At a first glance, these features are in contradiction to our results. This is caused by the fact that the MHD parameters Ha and N reached by both authors cover a completely different parameter range compared to our experiments (see Table 1), due to the very different material properties of the used liquid metals mercury and sodium, respectively. Thus, the electrical conductivity of sodium at a temperature of about 200°C is 7 to 8 times higher than the electrical conductivity of mercury at room temperature. The critical ratio of Ha/Re describing the threshold if the pressure drop follows the laminar behaviour at higher Ha numbers (see Eq. (3)), which is approximately 7×10^{-3} for an aspect ratio of one, was clearly exceeded in our experiments and not reached by Michiyoshi (1989). Another effect contradicting the bubble concentration by the influence of the magnetic field can be observed in a few void fraction distributions (for example, Fig. 7d and e). A rewidening of the distributions with increasing Hartmann number occurs. This fact is caused by the pinch effect connected with the existence of a pressure drop over the channel cross section due to the action of the induced magnetic field (see Moreau, 1990). A maximum of the pressure in the channel centre results in a drift of the gas bubbles towards the channel walls. An experimental evidence for that pinch effect was clearly provided by Saito et al. (1978a, 1978b). The authors concluded that the pinch effect becomes relevant for values of the Lundquist number $Lu = N \times Rm > 1$ (with magnetic Reynolds number $Rm = \mu\sigma_{el}VL$). However, a dominance of the pinch effect in our experiments can not be observed, although values of Lu up to 30 have been reached. The reason is that the influence of the wall conductance ratio c_w has also to be taken into account to describe the induced magnetic field as shown by Eckert (1997). In our experiment c_w is approximately 6 times lower compared to Saito et al. (1978a, 1978b), thus the void fraction distributions are not essentially influenced by the pinch effect.

3.2. Longitudinal magnetic field

In Fig. 9 we compare the bubble dispersion as observed in a transverse magnetic field (Section 3.1) to that obtained in a longitudinal field. The latter results are delivered from measurements in the mercury–nitrogen loop. Excluding the end regions where the field lines are

Table 1
Comparison of the nondimensional MHD parameter in the FZR experiment, Lykoudis (1985) and Michiyoshi (1989)

	Lykoudis (1985)	Michiyoshi (1989)	FZR experiment (present paper)
Fluid/gas	Hg/N_2	Hg/Ar	Na/Ar
Test section	Pipe (⌀ 38 mm)	Pipe (⌀ 23 mm)	Rectangular channel (45×50^2) mm
Wall material	Lucite	Lucite	Stainless steel
Re number	6.8×10^4–10^5	7×10^4–1.4×10^5	10^4–7×10^4
Ha_{max}	900	220	2700
$(Ha/Re)_{max} \times 10^3$	13	3	200
N_{max}	12	0.7	400
$(Lu = N \times Rm)_{max}$	0.2	0.01	30

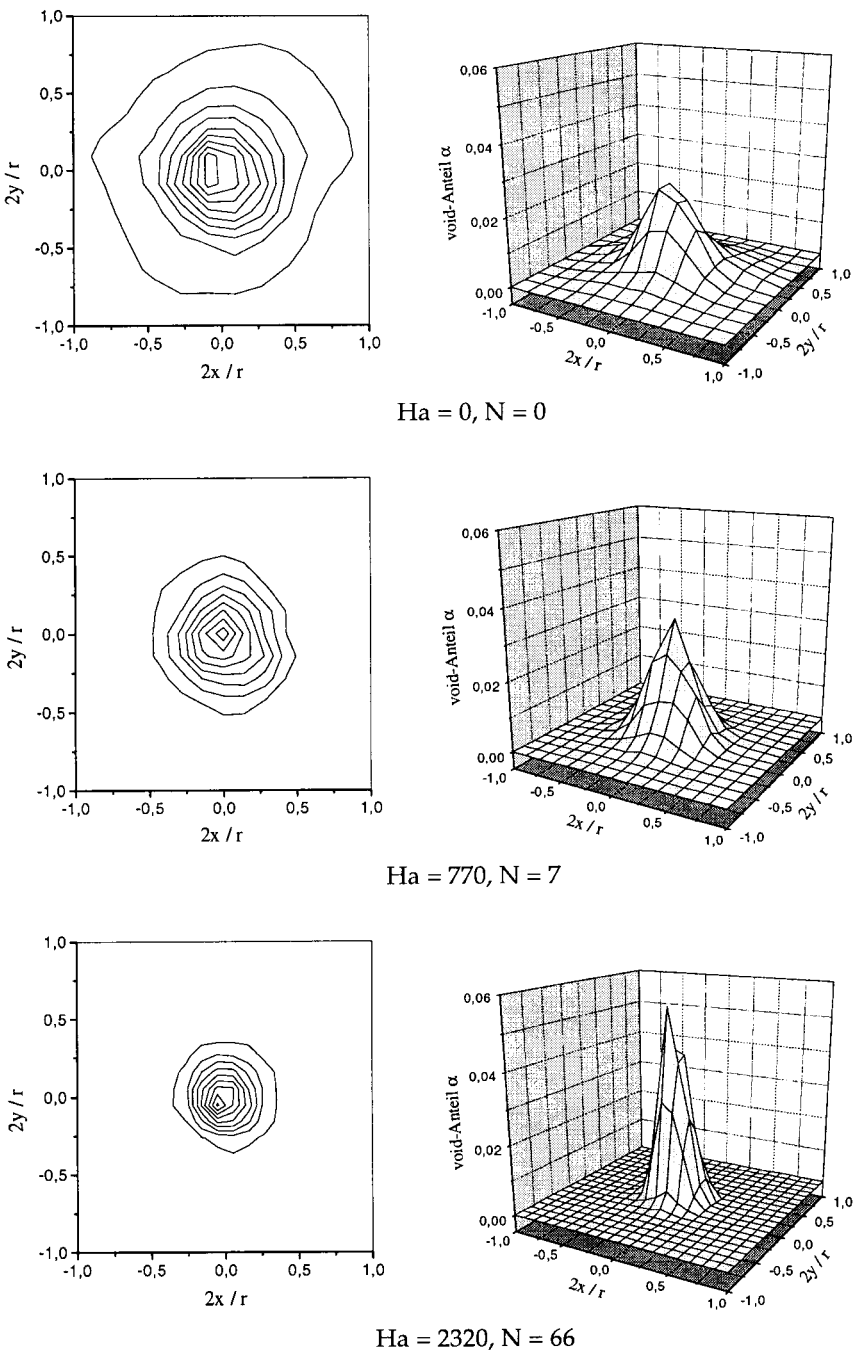

Fig. 9. Local void fraction distribution obtained at the mercury facility with a longitudinal magnetic field ($Re = 81600$).

not aligned with the mean flow, in the longitudinal magnetic field configuration no breaking of the axisymmetry occurs by the electromagnetic forces. We also find a significant concentration of the gas phase with growing field strength due to the electromagnetic damping of the turbulent fluctuations. Apart from that, the effect of both kind of magnetic fields on the flow structure is quite different. In contrast to the transverse case the void fraction distributions remain isotropic. Void fraction distributions obtained for other Reynolds numbers show the same qualitative behaviour.

Here, we do not encounter such a complex situation as shown in the transverse case, because the considered configuration with a longitudinal magnetic field is not suitable for the evolution of quasi-two-dimensional MHD turbulence. Vortices rotating in a plane perpendicular to the field direction are also affected by the electromagnetic damping process due to the absence of walls normal to the vorticity vector being able to prevent the closure of the induced electric currents.

4. Coefficients of turbulent dispersion

As a next step we wish to quantify the bubble transfer as function of the observed anisotropy in the transverse case. For this purpose we try to estimate dispersion coefficients in the direction parallel as well as perpendicular to the magnetic field from the experimental data.

The process of the bubble transfer is simply modelled by a two-dimensional diffusion equation for the local void fraction ϵ including a convective term in direction of the mean flow:

$$u_{\mathrm{G}}(z)\cdot\frac{\partial\epsilon}{\partial z}=D_x\cdot\frac{\partial^2\epsilon}{\partial x^2}+D_y\cdot\frac{\partial^2\epsilon}{\partial y^2} \tag{12}$$

The mean flow is considered as one-dimensional in the vertical z-direction and the magnetic field lines are directed parallel to the y-axis. Starting with a δ-function as initial distribution for ϵ in the plane $z=0$ we obtain the following solution for the void fraction ϵ:

$$\epsilon(x,y,z_{\mathrm{s}})=\frac{\dot{Q}_{\mathrm{G}}}{2\pi z_{\mathrm{s}}\sqrt{D_xD_y}}\cdot\exp\left(-\frac{1}{2}\cdot\frac{u_{\mathrm{G}}(x-x_0)^2}{z_{\mathrm{s}}D_x}\right)\cdot\exp\left(-\frac{1}{2}\cdot\frac{u_{\mathrm{G}}(y-y_0)^2}{z_{\mathrm{s}}D_y}\right) \tag{13}$$

where D_x and D_y are the dispersion coefficients along x- and y-axis, respectively, x_0,y_0 position of the bubble injection, z_{s} vertical probe position, and u_{G} the cross-sectional-averaged streamwise component of the bubble velocity.

Now, the determination of D_x and D_y is based on the following procedure: the experimental data of the void fraction along chordal lines in x- and y-direction are fitted to a gauss curve. With the assumptions

- constant gas flow rate $\dot{Q}_{\mathrm{G}}$ and constant bubble velocity u_{G} in the domain between the injection and the probe position,
- no significant pressure fluctuations

the dispersion coefficients can be calculated from the standard deviation of the fitted curves. The typical bubble velocity u_{G} for the corresponding experimental situation has been calculated

by a model especially developed for MHD bubbly flows. A detailed description of this model can be found in Eckert et al. (2000).

Together with the corresponding results of turbulence intensity measurements (Fig. 10a), the ascertained dispersion coefficients are displayed in Fig. 10b and c versus the MHD interaction parameter N. In both directions a significant reduction of the radial bubble transfer can be noted starting from the same level for $B = 0$ T. However, the direct comparison between the two curves for D_x and D_y reveals remarkable distinctions. While the gas dispersion along the magnetic field lines decreases sharply to values of 20–30% already at small values of the magnetic field, the decline of the dispersion coefficient perpendicular to the field direction occurs much more smoothly. Only if the magnetic field is strong enough ($Ha/Re \approx 0.3$) the gas bubble transfer becomes nearly equal in both directions. The distinct similarity between Fig. 10a and b indicates the existence of quasi-two-dimensional vortices in the flow being responsible for the transport of the gas bubbles perpendicular to the direction of the external magnetic field.

5. Conclusions

We have studied the dispersion of gas bubbles in a turbulent MHD flow. We find that the transport properties of the liquid metal two-phase flow are strongly modified due to the influence of an external magnetic field. An important feature in the parameter range of high Hartmann numbers consists in the significant damping of the turbulent motion crosswise to the mean flow direction. Therefore, a distinct concentration of the local distribution of a gas phase introduced by a single orifice is observed. Consequently, the dispersion coefficients determined for the case of a transverse magnetic field are reduced with increasing MHD interaction parameter N.

The electromagnetic force acts anisotropically. This is demonstrated by the fact that the damping of the turbulent bubble dispersion parallel to the magnetic field is much more pronounced than in the perpendicular direction. The decrease of the dispersion coefficient perpendicular to the magnetic field follows the corresponding dependence of the measured turbulence intensity on N. This is an indication that the mass transfer properties in this direction are determined by the existence of quasi-two-dimensional fluctuations in the flow.

For sufficiently large values of the Stuart number $N \approx 800$ a relaminarization of the flow is observed. The gas phase distribution is again isotropic and confined to a narrow channel region above the position of injection.

Due to the simplicity and the robustness of the measuring principle the employment of small gas bubbles as local tracers in liquid metal MHD flows is an efficient method for a qualitative monitoring of the turbulent structure. The limitations of this method become significant if the size of the gas bubbles is equal to or larger as the typical scale of the turbulence or if the character of the two-phase flow itself becomes too complex and determines the turbulent flow properties, for instance at too large gas contents or in complicated geometries.

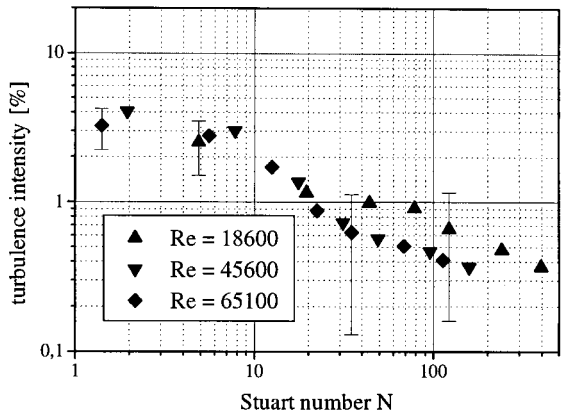

a) turbulence intensity versus N

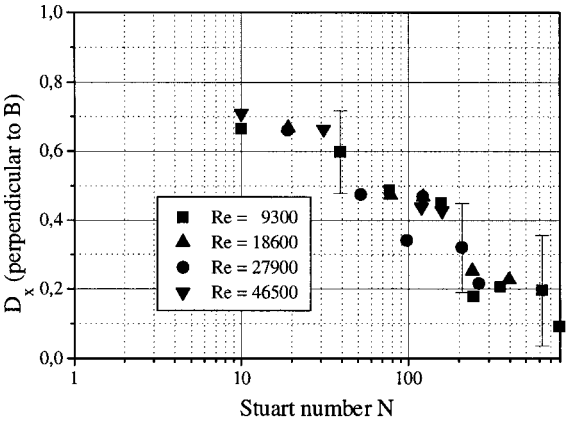

b) D_x versus N

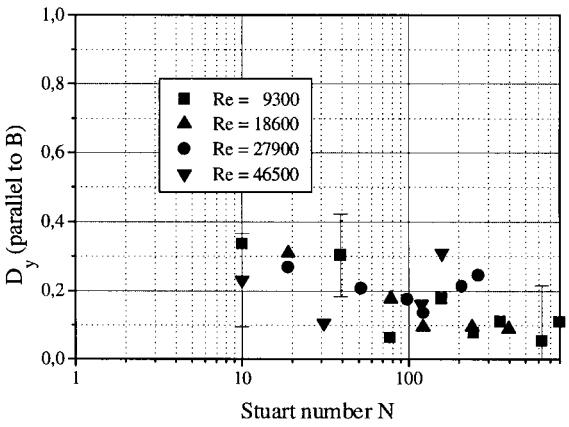

c) D_y versus N

Fig. 10. Comparison of the turbulence intensity and both estimated dispersion coeffients as functions of the MHD interaction parameter N.

Acknowledgements

This work was supported by the Deutsche Forschungsgemeinschaft under contract Ge 682/4-1. Furthermore, the authors would like to express their thanks to H. Langenbrunner, W. Witke, Y. Kolesnikov and E. Platacis for their valuable support in preparing and performing the experiments at both liquid metal facilities in Rossendorf and Riga, respectively.

References

Branover, H., 1978. Magnetohydrodynamic Flow in Ducts. Wiley, New York.

Branover, H., Eidelmann, A., Nagorny, M., 1994. Quasi-two-dimensional helical turbulence in MHD and geophysical flows. In: Proceedings of the Second International Conference on Energy Transfer in Magnetohydrodynamic Flows, Aussois, vol. 2, 777–785.

Brauer, H. 1971. Grundlagen der Einphasen- und Mehrphasenstroemungen. Sauerlaender, Aarau and Frankfurt/M.

Clift, R., Grace, J.R., Weber, M.E., 1978. Bubbles, Drops and Particles. Academic Press, New York.

Dunn, P.F., 1980. Single-phase and two-phase magnetohydrodynamic pipe flow. Int. J. Heat Mass Transfer 23, 373–385.

Eckert, S. 1997. Experimental investigations of turbulent liquid-metal and liquid-metal-gas flows in an external magnetic field. Ph.D. Thesis, Technical University Dresden.

Eckert, S., Gerbeth, G., Lielausis, O., 2000. The behaviour of gas bubbles in a turbulent liquid metal magnetohydrodynamic flow. Part II: Magnetic field influence on the slip ratio. Int. J. Multiphase Flow 26, 67–82.

Fabris, G., Dunn, P.F., Gawar, J.Z., Pierson, E.S., 1980. Local measurements in two-phase liquid metal MHD. In: Proceedings of the Second Beer-Sheva Seminar, Jerusalem, 1978. Israel University Press, Jerusalem, 157–171.

Gherson, P., Lykoudis, P.S., 1984. Local measurements in two-phase liquid-metal magneto-fluid-mechanic flows. J. Fluid Mech 147, 81–104.

Hinze, O., 1955. Fundamentals of the hydrodynamic mechanisms of splitting in dispersion process. Journal of AIChE 1, 289–295.

Jones, O.C., Delhaye, J.-M., 1976. Transient and statistical measurement techniques for two-phase flows: A critical review. Int. J. Multiphase Flow 3, 89–116.

Kraichnan, R.H., 1967. Inertial ranges in two-dimensional turbulence. Phys. Fluids 10, 1417–1423.

Kolesnikov, Y.B., Tsinober, A.B., 1974. Experimental investigation of two-dimensional turbulence behind a grid. Izv. Akad. Nauk SSSR Mekh. Zh. i Gaza 4, 146–150.

Lykoudis, P.S., 1985. Liquid metal magneto-fluid-mechanic turbulence. Proceedings of the Fourth Beer-Sheva Seminar, Jerusalem, 1984. AIAA 100, 255–279.

Lykoudis, P.S., Revankar, S.T., Black, D.B., 1994. Suppression of bubble-induced turbulence in the presence of a magnetic field. Proceedings of the Seventh Beer-Sheva Seminar, Jerusalem, 1993. AIAA 162, 121–129.

Michiyoshi, I., 1989. Liquid metal two-phase flow heat transfer with and without magnetic field. JSME Int. Journal 32, 483–493.

Michiyoshi, I., Fanakawa, H., Kuramoto, C., Akita, Y., Takahashi, O., 1977. Local properties of vertical mercury–argon two-phase flow in a circular tube under transverse magnetic field. Int. J. Mutiphase Flow 3, 445–457.

Michiyoshi, I., Serizawa, A., 1984. Turbulence in two-phase bubbly flow. In: Proceedings of the Japan-U.S. Seminar on Two-Phase Flow Dynamics, Lake Placid.

Moreau, R., 1990. Magnetohydrodynamics. Kluwer, Dordrecht.

Mori, Y., Hijikata, K., Kuriyama, I., 1977. Experimental study of bubble motion in mercury with and without magnetic field. J. Heat Transfer Trans. ASME 99, 404–410.

Ohba, K., Yuhara, T., 1979. Study of turbulence structure in a vertical square duct flow of a bubbly mixture using LDV. In: Second Multiphase Flow and Heat Transfer Symposium, Miami.

Panidis, T., 1995. On the evaluation of autocorrelation and power spectrum in dispersed two-phase flows. In: International Symposium on Measuring Techniques for Multiphase Flows, Nanjing, China.

Saito, M., Nagae, H., Inoue, S., Fujii-E, Y., 1978a. Redistribution of gaseous phase of liquid metal two-phase flow in a strong magnetic field. J. Nucl. Sci. Technol 15, 729–735.

Saito, M., Inoue, S., Fujii-E, Y., 1978b. Gas-liquid slip ratio and MHD pressure drop in two-phase liquid metal flow in strong magnetic field. J. Nucl. Sci. Technol 15, 476–489.

Serizawa, A., Ida, T., Takahashi, O., Michiyoshi, I., 1990. MHD effect on NaK-nitrogen two-phase flow and heat transfer in a vertical round tube. Int. J. Mutiphase Flow 16, 761–788.

Serizawa, A., Kataoka, I., Michiyoshi, I., 1975a. Turbulence structure of air–water bubbly flow. Part I: Measuring techniques. Int. J. Multiphase Flow 2, 221–234.

Serizawa, A., Kataoka, I., Michiyoshi, I., 1975b. Turbulence structure of air–water bubbly flow. Part II: Local properties. Int. J. Multiphase Flow 2, 235–246.

Serizawa, A., Kataoka, I., Michiyoshi, I., 1975c. Turbulence structure of air–water bubbly flow. Part III: Transport properties. Int. J. Multiphase Flow 2, 247–259.

Sevik, M., Park, S.H., 1973. The splitting of drops and bubbles by turbulent fluid flow. ASME Journal of Fluids Engineering 3, 53–60.

Sommeria, J., Moreau, R., 1982. Why, how, and when MHD turbulence becomes two-dimensional. J. Fluid. Mech 118, 507–518.

Sullivan, J.P., Houze, R.N., Buenger, D.E., Theofanous, T.G., 1978. Turbulence in two-phase flows. In: U.E.C.D., C.S.W.I., Paris.

Taylor, G.I., 1934. The formation of emulsion in definable field of flow. Proceedings of the Royal Society London, Series A 146, 501.

Thome, R.J. 1964. Effect of a transverse magnetic field on vertical two-phase flow through a rectangular channel. Argonne National Laboratory Report, ANL-6854.